THIN FILM SILICON EMITTERS FOR CRYSTALLINE SILICON SOLAR CELLS, EPITAXIAL, AMORPHOUS OR MICROCRYSTALLINE ? - A SIMULATION STUDY

R.Stangl*, A.Froitzheim, W.Fuhs
Hahn-Meitner-Institut Berlin, Abt. Silizium Photovoltaik, Kekuléstr. 5, D-12489 Berlin
*corresponding author: Dr. Rolf Stangl, Tel: +49/30/67053-312, Fax: ~333, e-mail: stangl@hmi.de

ABSTRACT: The performance of solar cells which consist of thin-film silicon emitters of the type epi-Si(n), a-Si(n)/a-Si(i) or µc-Si(n)/a-Si(i) grown on a high quality p-type silicon wafer, is investigated by numerical computer simulation. The influence of the emitter/wafer interface state density, of the front contact surface recombination velocity and of the front contact barrier height on the IV-characteristics of the solar cells is examined. It is shown that applying a TCO as a front contact material, severe degradation of the solar cell performance is to be expected in case of an epi(n) and an a-Si(n)/a-Si(i) emitter due to emitter depletion and reduction of the internal field within the c-Si absorber. It is shown that a µc-Si(n)/a-Si(i) emitter offers some advantages: (1) The cell is almost insensitive to the TCO/emitter contact, and (2) its higher doping efficiency leads to higher short circuit currents and to a better suppression of the emitter/wafer interface recombination.

KEYWORDS: c-Si (1), Si-films (2), heterojunction (3)

1. INTRODUCTION

Silicon solar cells with thin-film emitters deposited at low temperature from the gas phase onto Si-wafers offer an interesting technological alternative to conventional crystalline silicon solar cell technology with diffused p/n junctions. Such emitters can be realized by epitaxially grown silicon films (epi-Si) [1,2], microcrystalline (µc-Si) [2] or amorphous silicon (a-Si) [3,4]. Processing is comparatively simple and does not require high temperature steps. The most successful route so far has been the amorphous Si emitter technology which has led to 20.7 % efficiency in the laboratory and which is about to be industrialized by Sanyo [4]. The performance of these type of solar cells critically depend on the successful suppression of the emitter/wafer interface recombination.

The three different device structures that are considered here are sketched in Fig. 1. An ultra thin-film silicon emitter with a typical thickness of 5 - 30 nm is deposited on top of a moderately p-doped, monocrystalline silicon wafer. The n-doped emitter can be grown either (a) epitaxially, (b) amorphous or (c) microcrystalline. An intrinsic buffer layer of amorphous silicon will additionally be used in case of amorphous or microcrystalline emitters in order to achieve a good emitter/wafer interface passivation. The moderate sheet resistivity of the thin film emitter requires the use of a transparent, conductive layer (TCO) as a front contact. In addition high-efficiency-features may be used such as surface texturing and a back surface field.

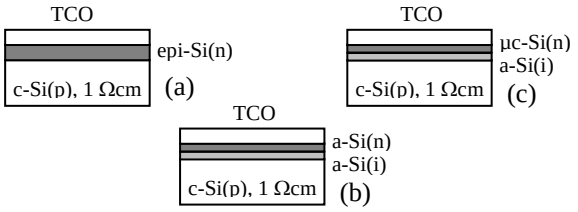

Fig.1: Three possible device structures of a silicon solar cell realised by a gas-phase deposited n-type thin-film silicon emitter on a p-type wafer.

The performance of such a 'thin-film-silicon-emitter-on-silicon' solar cell critically depends on the recombination at the emitter/wafer interface. Such recombination losses can directly be suppressed by ensuring a low density of states at the interface, but also by a strong band bending in the crystalline wafer, which leads to an inversion layer at the interface [5]. Of crucial importance is the influence of the TCO front contact. This contact between a silicon emitter and the TCO can drive the emitter into depletion. For thin emitter layers this will also affect the band bending in the crystalline wafer.

Considering the three device structures (Fig.1), the interfaces of the emitter/wafer and the TCO/emitter will of course affect the solar cell performance in a different way. It is still an open question, which structure should be preferred at least from a theoretical point of view. In this paper the three structures are compared by means of a numerical computer simulation with particular emphasis on the influence of the emitter/wafer interface state density, the TCO/emitter recombination velocity and the TCO/emitter barrier height on the solar cell characteristic (V_{oc}, I_{sc}, fill factor and efficiency).

2. MODELLING

The one-dimensional, algebraic semiconductor equations have been solved numerically using Shockley-Read-Hall recombination statistics. For the individual layers as well as for the emitter/wafer interfaces particular defect state distributions are specified.

	epi-Si(n)	**a-Si(n)**	**µc-Si(n)**
band gap [eV]	1.12	[1.7 – 1.8]	[1.3 – 1.5]
absorption	low	high	moderate
defect density [cm^{-3}]	$\approx 10^{13}$	$\approx 10^{18}$	$\approx 10^{17}$
mobility [cm^2/Vs]	≈ 60	≈ 1	≈ 2
Maximum hole diffusion length [nm]	≈ 4000	≈ 5	≈ 20
activation energy [eV]	→ 0	≥ 0.2	→ 0

Table 1: main differences of the electronic properties of the n-doped silicon emitter layers of figure 1.

In order to compare the three different device structures of Fig. 1 the total emitter thickness of epi-Si(n), a-Si(n)/a-Si(i) or µc-Si(n)/a-Si(i) is kept constant at 10 nm if not stated otherwise. If there is an intrinsic buffer layer, the thickness of the intrinsic layer is assumed to be equal to the thickness of the doped layer (5 nm if not stated otherwise). The TCO front contact is modelled by specifying the TCO/emitter surface recombination velocity S_{front} and the TCO/emitter barrier height ϕ_{front}. A reflection and absorption loss of 20% of the incident solar radiation is assumed, which is a typical value of flat substrates (no surface texturing) together with a TCO thickness of 80 nm. If not stated otherwise, there is no back surface field.

For the crystalline c-Si(p) absorber, a doping concentration of $N_a = 1.5\ 10^{16} cm^{-3}$ and a constant defect state distribution of $D = 10^{11} cm^{-3}\, eV^{-1}$ was assumed. This corresponds to a high quality FZ wafer (1 Ωcm) with a minority carrier diffusion length of $L_e = 500\,\mu m$, a value which is larger than the wafer thickness of 300 µm.

For the amorphous silicon layers, a-Si(n) and a-Si(i), a band gap of $E_g = 1.72\,eV$ and an electron affinity of $\chi = 3.8\,eV$ was assumed. For the doped films the doping concentration was set to $N_d = 10^{19} cm^{-3}$. The defect-state distributions within the band gap are exponential band tail states and Gaussian dangling bond states. These data are taken from literature [6] and are sketched in Fig. 2. These parameters result in an activation energy of $E_A = 0.25\,eV$ in case of doped a-Si(n) and $E_A = 0.82\,eV$ in case of intrinsic a-Si(i), see Fig 2.

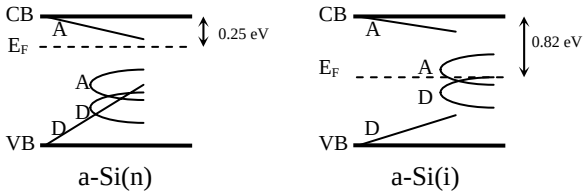

Fig. 2: Sketch of the acceptor-like (A) and donor-like (D) defect-state distributions of a-Si:H(n) and a-Si:H(i) used in the simulation.

For the microcrystalline silicon layer, µc-Si(n), a band gap of $E_g = 1.3\,eV$ and an electron affinity of $\chi = 3.8\,eV$ was assumed. The defect-state distributions are a constant distribution, $D = 10^{15} cm^{-3}\, eV^{-1}$, and tail states [6] (Fig. 3). Assuming a doping concentration of $N_d = 10^{19} cm^{-3}$ the resulting activation energy is $0.03\,eV$. In case of an epitaxial silicon layer, epi-Si(n), the band gap and the electron affinity are taken as for crystalline Silicon ($E_g = 1.12\,eV$ and $\chi = 4.05\,eV$). There are no tail states and the defect-state distribution is considered to be constant ($D = 10^{13} cm^{-3}\, eV^{-1}$).

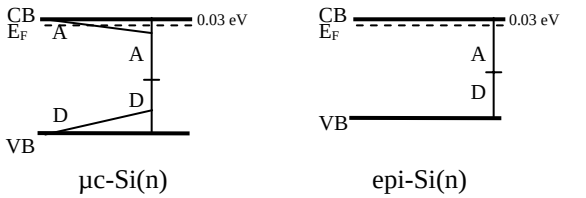

Fig. 3: Sketch of the acceptor-like (A) and donor-like (D) defect-state distributions of µc-Si(n) and epi-Si(n).

Table 1 lists the main differences of the parameters of the different n-type silicon emitter layers. Among the silicon emitter layers amorphous silicon has the highest band gap. At a first inspection, this should be advantageous, since the defect-rich thin film emitter then basically serves as a window layer. However, the absorptivity of amorphous silicon is much higher compared to µc-Si or epi-Si, such that in case of the µc-Si emitter the fewest photons are absorbed in the doped emitter parts.

Considering the defect density within the emitter layers, the epi(n) emitter has significantly less defects. Thus, in case of using the epi(n) emitter, the resulting maximum obtainable minority carrier diffusion length L_h is much larger than the emitter thickness. Charge carriers generated within the epi-Si(n) can therefore contribute to the total current of the solar cell. In case of the a-Si(n)/a-Si(i) or µc-Si(n)/a-Si(i) emitters, L_h is in the order of the emitter thickness. Therefore, in a first approximation charge carriers generated within the doped parts of these emitters will not contribute to the total current. However, charge carriers generated within the intrinsic parts of the emitter can be collected due to the built in electric field of the device (nip-structure).

Finally, the doping efficiency of a-Si(n) is restricted, the activation energy of the dark conductivity (the energetic distance $E_C - E_F$ between the conduction band and the Fermi energy) is limited to values of above $200\,meV$. This is not the case for µc-Si(n) or epi-Si(n), where it is possible to dope even beyond the semiconductor metal transition $E_C - E_F = 0$. Thus with an epi-Si(n) or a µc-Si(n)/a-Si(i) emitter the build in potential and the band bending in the crystalline c-Si(p) absorber can be enhanced considerably.

3. BAND DIAGRAMS AND I-V CHARACTERISTICS

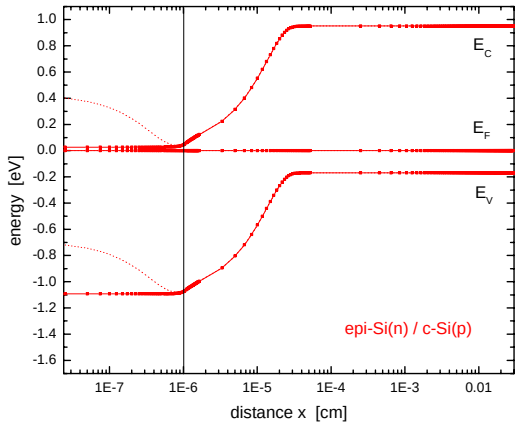

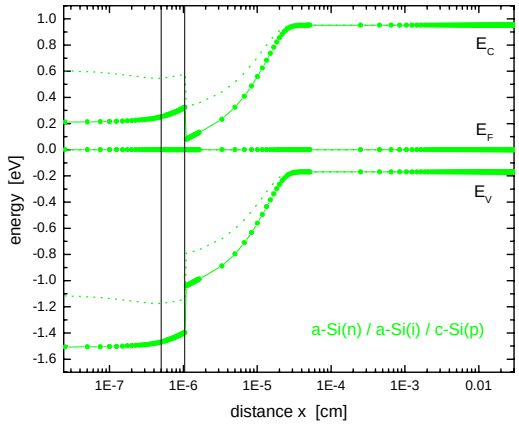

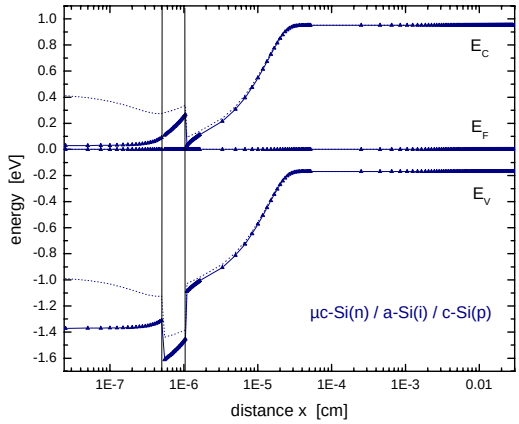

Fig. 4: Band profiles of the three different device structures. With respect to the TCO/emitter front contact, the band diagrams are calculated under zero barrier height (flatband conditions, straight lines) and assuming a barrier height of 0.4 eV (emitter depletion, dotted lines). The position is given in logarithmic scale, the TCO contact is on the left at x=0 cm, the Fermi energy was set to 0 eV on the energetic scale.

Fig.4 displays the resulting band profiles for the three device structures. In a first approximation, additional interface defects at the emitter/wafer interface have been neglected. Further assumptions are flat band conditions ($\phi_{front} = 0\ eV$) and a high recombination velocity ($S_{front} = 10^7$ cm/s) at the TCO/emitter interface. Also shown is the influence of a positive front contact barrier height of $\phi_{front} = 0.4\ eV$, which drives the emitter into depletion.

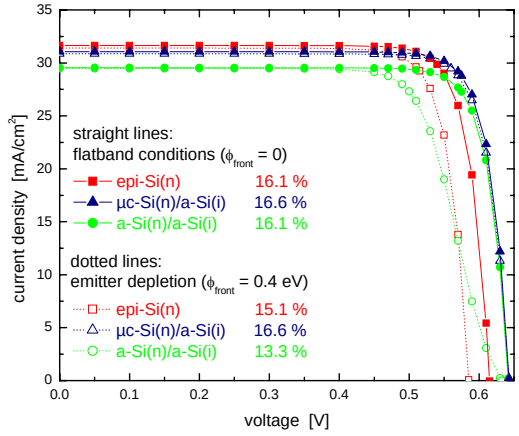

Fig. 5: Simulated I-V curves of 'thin-film-silicon-emitter-on-p-doped silicon' solar cells with epi-Si(n), μc-Si(n)/a-Si(i) and a-Si(n)/a-Si(i) emitters on flat substrates (reflection loss of 20 %) and without back surface field. The curves are calculated for zero barrier height (flatband conditions, straight lines) and for a barrier height of 0.4 eV (emitter depletion, dotted lines) at the TCO/emitter front contact.

Fig. 5 displays the simulated I-V characteristics under illumination with AM 1.5 light. The resulting cell efficiencies exceed 16 % for all device structures. If high efficiency features were taken into account including a back surface field and only 3 % reflection loss the resulting efficiencies would exceed 21 %.

Four characteristic features are observed which remain, even if the defect density at the emitter/wafer interface and/or the front contact barrier height at the TCO/emitter interface is varied: (1) The solar cell efficiency is always highest for the μc-Si(n)/a-Si(i) emitter. (2) Under variation of the front contact barrier height the IV-characteristic does not change significantly in case of the μc-Si(n)/a-Si(i) emitter, whereas the solar cell efficiency degrades significantly for higher barrier heights in case of the epi-(n) and a-Si(n)/a-Si(i) emitters. (3) The short-circuit current decreases in the sequence from epi-Si(n) to μc-Si(n)/a-Si(i) and to a-Si(n)/a-Si(i). (4) The open-circuit voltage is significantly reduced for the epi-Si(n) emitter. The physical origin of this features will now be examined in more detail.

The reason for the trend in the decrease of the short-circuit current is simple: Most photons absorbed in the epi-Si(n) emitter will contribute to the short-circuit current, whereas the doped parts of the other two emitters are electrically dead in first approximation. Due to the higher built-in-potential of the μc-Si(n)/a-Si(i) emitter compared to the a-Si(n)/a-Si(i) emitter more charge carriers generated in the emitter will be collected in case of the μc-Si(n)/a-Si(i) emitter. In order to explain the other three characteristic features mentioned above, the influence of the emitter/wafer interface and of the TCO/emitter interface on the solar cell performance has to be discussed in more detail for all three emitter types.

4. EMITTER/WAFER INTERFACE STATE DENSITY

Interface states at the emitter/wafer interface will significantly reduce the open-circuit voltage of the solar cell (Fig. 6). A constant interface state distribution throughout the c-Si band gap has been used for simulation. The reduction in open-circuit voltage is due to additional interface recombination and can be partially suppressed by ensuring a strong band bending in the crystalline c-Si(p) absorber, as shown in [5], [7] for an a-Si(n)/a-Si(i) emitter. In any case, it is essential to passivate the emitter/wafer interface in a way that defect densities not larger than $N_{trap} = 10^{12}$ cm^{-2} are achieved (see Fig. 6). This appears possible making use of the excellent passivation that can be achieved with an a-Si(i) buffer layer [8].

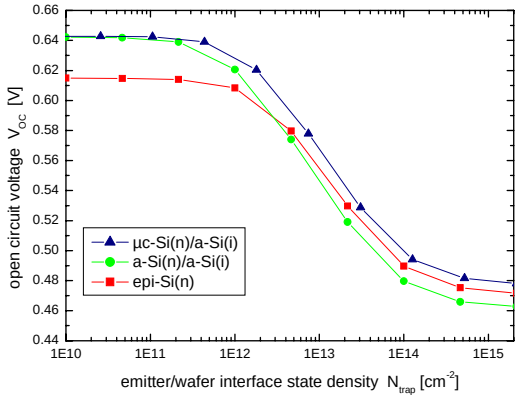

Fig. 6: Dependence of the open-circuit voltage V_{OC} on the emitter/wafer interface state density for epi-Si(n), μc-Si(n)/a-Si(i) and a-Si(n)/a-Si(i) emitters.

TCO/EMITTER SURFACE RECOMBINATION VELOCITY

Good surface passivation of the TCO/emitter surface is only necessary in case of the epi-Si(n) emitter (see Fig. 7). If the front surface recombination velocity is reduced from $S_{front} = 10^7$ cm/s to 10^3 cm/s, a higher open-circuit voltage

can be obtained only in case of the epi-Si(n) emitter. This is due to the fact that the doped parts of the µc-Si(n)/a-Si(i) and the a-Si(n)/a-Si(i) emitters are electrically dead especially close to the TCO/emitter interface. The short-circuit current and fill factor remain essentially unchanged for all emitter types.

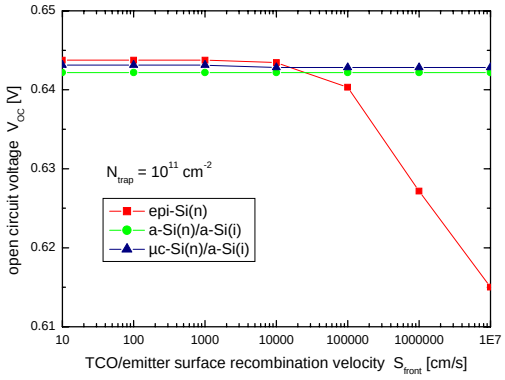

Fig. 7: Dependence of the open-circuit voltage V_{OC} on the TCO/emitter surface recombination velocity for epi-Si(n), µc-Si(n)/a-Si(i) and a-Si(n)/a-Si(i) emitters.

5. TCO/EMITTER BARRIER HEIGHT

According to Andersons model, the TCO/emitter contact will always drive the emitter into depletion [7]. This has also been investigated experimentally in case of the TCO/a-Si(n) contact [9]. According to this work the TCO/emitter front contact barrier height is expected to be somewhere in the range 0.2 – 0.4 eV depending on the value of the TCO work function and the type of contact.

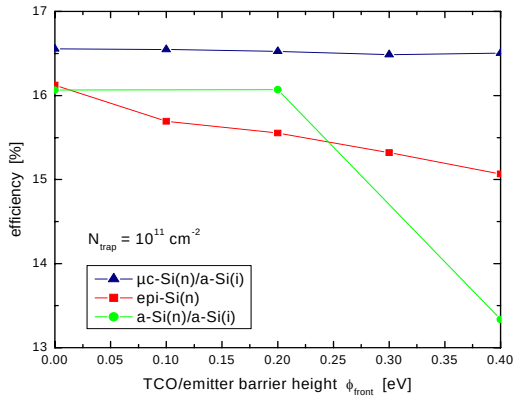

Fig. 8: Dependence of the solar cell efficiency on the TCO/emitter barrier height of epi-Si(n), µc-Si(n)/a-Si(i) and a-Si(n)/a-Si(i) emitters.

Again, for the µc-Si(n)/a-Si(i) emitter, the solar cell efficiency remains approximately unaffected by the TCO/emitter barrier height (see Fig. 8). With an a-Si(n)/a-Si(i) emitter, mainly the fill factor but also the open-circuit voltage decreases. For the epi-Si(n) emitter there is a slight decrease of the open-circuit voltage and also of the short-circuit current. This leads to the decrease in solar cell efficiency as shown in Fig. 8.

If the doped part of the emitter is thick enough, the free carriers of the emitter will be sufficient to shield the electric field imposed by the TCO/emitter front contact barrier height. This will only affect the solar cell performance in case of the epi-Si(n) emitter, since the doped parts of the µc-Si(n)/a-Si(i) and the a-Si(n)/a-Si(i) emitters are electrically dead. However, if the emitter is sufficiently thin, additional carriers from the absorber and recharged defects from the emitter have to be used in order to shield the electric field. This will considerably alter the band bending in the crystalline c-Si(p) absorber of the solar cell, and lead to a strong decrease of the fill factor and the open-circuit voltage. With an emitter thickness of $10\,nm$, this critical value for the thickness has already been reached in case of the a-Si(n)/a-Si(i) emitter, but not in case of the epi-Si(n) or the µc-Si(n)/a-Si(i) emitters (see Fig.4 for comparison). The reason for this is the limitation of the doping efficiency of a-Si(n). Therefore, for reasonably thin emitter layers in the range of 3 – 30 nm, only the µc-Si(n)/a-Si(i) emitter is insensitive to the TCO/emitter barrier height. Note that a reasonably thin emitter is required for good solar cell performance in order to minimize absorption losses in the emitter layers.

6. CONCLUSION

The simulation study leads to detailed insight into the physical background and limitations of 'thin-film-silicon-emitter-on-p-doped silicon' solar cells using gas-phase deposited emitters of the type epi-Si(n), µc-Si(n)/a-Si(i) and a-Si(n)/a-Si(i). It turns out hat excellent emitter/wafer interface passivation which leads to defect densities of less than $N_{trap} = 10^{12}\,cm^{-2}$ is of crucial importance. With the exception of the µc-Si(n)/a-Si(i) emitter, a positive TCO/emitter barrier height, which is to be expected using a TCO/thin film silicon contact, severely degrades the solar cell performance. In particular for the epi-Si(n) emitter the TCO/emitter surface recombination velocity has to be controlled ($S_{front} \le 10^4$ cm/s). This simulation study suggests that the µc-Si(n)/a-Si(i) emitter may have some advantages over the other choices: (1) This emitter is insensitive to the TCO/emitter front contact and (2) the high doping efficiency of µc-Si(n) leads to a stronger band bending in the absorber. The latter may result in a pronounced reduction of the emitter/absorber interface recombination and also to a higher yield of charge carriers, which are absorbed within the emitter.

REFERENCES

[1] K.Lips, J.Platen, S.Christiansen, I.Sieber, L.Elstner, W.Fuhs, Proc.28th IEEE PVSEC (2000, Alaska), 61.

[2] R.Rizzoli, E.Centurioni, J.Pla, C.Summonte, A.Migliori, A.Desalvo, F.Zignani, J.Non-Cryst.Solids, 299-302 (2002) 1203.

[3] N.Jensen, R.M.Hausner, R.B.Bergmann, J.H.Werner, U.Rau, Prog.Photovolt., 10, (2002), 1.

[4] H.Sakata, T.Nakai, T.Baba, M.Taguchi, S.Tsuge, K.Uchihashi, S.Kiyama, Proc. 20th IEEE PVSEC (2000), 7.

[5] R.Stangl, A.Froitzheim, L.Elstner, W.Fuhs, Proc. 17th EUR PVSEC, (2001, Munich).

[6] R.Schropp, M.Zeman, Amorphous and Microcrystalline Silicon Solar Cells, Kluwer Academic Publishers (1998).

[7] A.Froitzheim, R.Stangl, L.Elstner, M.Schmidt, W.Fuhs, Proc. 29th IEEE PVSEC (2002, New Orleans).

[8] S.Dauwe, J.Schmidt, R.Hetzel, Proc. 29th IEEE PVSEC (2002, New Orleans).

[9] M.Schmidt, A.Froitzheim, R.Stangl, L.Elstner, K.Kliefoth, W.Füssel, M.Schmidt, W.Fuhs, Proc. 17th EUR PVSEC, (2001, Munich).